buildings

MDPI

Article

Feasibility of Advanced Reflective Cracking Prediction and Detection for Pavement Management Systems Using Machine Learning and Image Detection

Sung-Pil Shin [1], Kyungnam Kim [2,*] and Tri Ho Minh Le [3,*]

[1] Department of Highway & Transportation Research, Korea Institute of Civil Engineering and Building Technology, 283 Goyandae-ro, Ilsanseo-gu, Goyang-si 10233, Republic of Korea; spshin@kict.re.kr
[2] Pavement Research Division, Korea Expressway Corporation Research Institute, Dong-tansunhwan-daero 17-gil, Hwaseong-si 18489, Republic of Korea
[3] Faculty of Civil Engineering, Nguyen Tat Thanh University, 300A Nguyen Tat Thanh Street, District 4, Ho Chi Minh City 70000, Vietnam
* Correspondence: kkn248@ex.co.kr (K.K.); lhmtri@ntt.edu.vn (T.H.M.L.)

Abstract: This research manuscript presents a comprehensive investigation into the prediction and detection of reflective cracking in pavement infrastructure through a combination of machine learning approaches and advanced image detection techniques. Leveraging machine learning algorithms, reflective cracking prediction models were developed and optimized for accuracy and efficiency. Additionally, the efficacy of image detection methods, particularly utilizing Mask R-CNN, was explored for robust and precise identification of reflective cracking on pavement surfaces. The study not only aims to enhance the predictive capabilities of pavement management systems (PMSs) through machine learning-based models but also seeks to integrate advanced image detection technologies to support real-time monitoring and assessment of pavement conditions. By providing accurate and timely detection of reflective cracking, these methodologies contribute to the optimization of pavement maintenance strategies and the overall improvement of pavement infrastructure management practices. Results indicate that the developed machine learning models achieve an average predictive accuracy of over 85%, with some models achieving accuracies exceeding 90%. Moreover, the utilization of a mask region-based convolutional neural network (Mask R-CNN) for image detection demonstrates exceptional precision, with a detection accuracy of over 95% on average across different pavement types and weather conditions. The results demonstrate the promising performance of the developed machine learning models in predicting reflective cracking, while the utilization of Mask R-CNN showcases exceptional accuracy in the detection of reflective cracking from images. This research underscores the importance of leveraging cutting-edge technologies to address challenges in pavement infrastructure management, ultimately supporting the sustainability and longevity of transportation networks.

Keywords: reflective cracking prediction; machine learning algorithms; image detection techniques; mask R-CNN; pavement management systems

check for updates

Citation: Shin, S.-P.; Kim, K.; Le, T.H.M. Feasibility of Advanced Reflective Cracking Prediction and Detection for Pavement Management Systems Using Machine Learning and Image Detection. *Buildings* **2024**, *14*, 1808. https://doi.org/10.3390/buildings14061808

Academic Editor: Pengfei Liu

Received: 10 May 2024
Revised: 2 June 2024
Accepted: 13 June 2024
Published: 14 June 2024

Copyright: © 2024 by the authors. Licensee MDPI, Basel, Switzerland. This article is an open access article distributed under the terms and conditions of the Creative Commons Attribution (CC BY) license (https://creativecommons.org/licenses/by/4.0/).

1. Introduction

The construction and maintenance of road infrastructure are vital for facilitating economic development and ensuring safe transportation systems [1]. However, roads are susceptible to various environmental factors and climatic conditions that can lead to pavement distress [2], including reflective cracking. Reflective cracking, a prevalent form of pavement distress, poses significant challenges to the durability and performance of road infrastructure [3]. These cracks typically originate from underlying cracks or joints in the pavement structure and propagate upwards [4], often exacerbated by factors such as temperature fluctuations, traffic loading, and moisture infiltration [5]. The formation of

reflective cracks is a complex phenomenon influenced by various factors, including pavement design, material properties, construction practices, and environmental conditions [6]. Asphalt overlays placed on existing pavements, especially those with jointed or severely cracked substrates, are particularly susceptible to reflective cracking over time [7]. These cracks not only compromise the structural integrity of the pavement but also serve as pathways for water penetration, leading to further deterioration and pavement degradation [8]. Managing reflective cracking is critical for ensuring the longevity and functionality of road networks, as untreated cracks can result in increased roughness, reduced ride quality, and safety hazards for road users [9]. Therefore, developing effective detection and mitigation strategies for reflective cracking is essential for the sustainable management of pavement assets and the efficient allocation of maintenance resources within pavement management systems (PMSs).

Managing reflective cracking is paramount for the effectiveness of pavement management systems (PMSs) [10,11], which are responsible for optimizing the allocation of maintenance and repair (M&R) funds to ensure the longevity and functionality of road networks. Identifying and addressing reflective cracking promptly is essential to prevent further deterioration and costly repairs [12,13]. However, traditional detection methods may not always be efficient or accurate in identifying reflective cracking, especially in diverse environmental conditions [14].

To support PMS in effectively managing reflective cracking, there is a growing need for smarter detection techniques that leverage advanced technologies such as deep learning and image processing [14]. By developing automated and intelligent systems capable of detecting reflective cracking with high accuracy and efficiency [15,16], government agencies can streamline maintenance and rehabilitation (M&R) efforts and allocate resources more effectively [17,18]. A smarter way to navigate and track reflective cracking not only enhances road safety but also optimizes the utilization of public funds, ensuring sustainable infrastructure management for the long term [19,20].

Advances in inexpensive and excellent-quality imaging sensors have played a major role in the remarkable development of the application of computer vision approaches inside civil engineering research in recent years [18,21]. With the use of these methods, it is possible to take precise digital pictures of pavement surfaces [22], which presents chances to identify important markers for evaluating the state of the pavement, such as corrosion, debonding, fractures, and spalling. The capacity of machine vision to perform comprehensive, non-contact, economical, unbiased, and computerized state evaluations is one of its main benefits in this situation [23].

Recent advancements in deep learning algorithms have transformed vision-based pavement damage detection [24,25], offering improved efficiency and reliability [26]. These advancements have enabled the development of sophisticated image segmentation techniques that can accurately identify and classify various types of pavement distress, including reflective cracking [27,28]. Technique features include automated crack detection and reduction in human biases and errors [29,30]. Object detection, crucial for civil engineering infrastructure maintenance and safety, has seen significant progress with algorithms like YOLOv6, v7, and v8, each introducing new features and improved performance [31–34]. Deep learning-based techniques, such as Faster R-CNN, have shown success in various applications, including road deterioration classification. Diverse augmentation methods are recommended to further enhance accuracy [34–36].

This research manuscript presents a comprehensive investigation into the prediction and detection of reflective cracking in pavement infrastructure through a combination of machine learning approaches and advanced image detection techniques. Leveraging machine learning algorithms, reflective cracking prediction models were developed and optimized for accuracy and efficiency [22]. Additionally, the efficacy of image detection methods, particularly utilizing Mask R-CNN [22], was explored for robust and precise identification of reflective cracking on pavement surfaces. The study not only aims to enhance the predictive capabilities of PMS through machine learning-based models but

also seeks to integrate advanced image detection technologies to support real-time monitoring and assessment of pavement conditions [37–39]. By providing accurate and timely detection of reflective cracking, these methodologies contribute to the optimization of pavement maintenance strategies and the overall improvement of pavement infrastructure management practices [40–42].

This study proposes the use of an advanced learning model to classify images of "reflective cracking zones" across various pavement textures and weather conditions. The aim is to enhance pavement management systems (PMSs) by monitoring reflective cracking for maintenance purposes, thereby reducing associated risks. This approach covers different pavement types, including both asphalt and concrete conditions. The primary goal is to develop a robust computational model capable of handling a wide range of inspection tasks while remaining resilient to variations in photographic conditions. To achieve this, a dataset comprising 1280 images was utilized for algorithm training. These images were sourced from multiple platforms, including the Internet, on-site pavement surveys conducted in South Korea, and Google Street View. Data augmentation techniques were employed to enhance diversity, and the dataset was split into 80% for training and 20% for cross-validation. The research progressed through two pivotal stages: first through the development of a Convolutional Neural Network (CNN) architecture for the classification of reflective cracking, and second through the implementation of an image segmentation technique for reflective cracking detection, followed by an analysis of the training dataset.

2. Methodology

2.1. Development of Deep Learning Prediction Models for Reflective Cracking in Highways

2.1.1. Overview

This section explores the development of deep learning prediction models for reflective cracking in highways, focusing on both empirical and analytical approaches. The objective is to forecast reflective crack occurrences by considering weather and traffic statistics. The predictive model, which combines separate variables and coefficients, is designed to assess and manage the risk of reflective cracking, crucial for enhancing pavement maintenance strategies. Supervised learning methods for machine learning forecasting, including decision trees, multiple regression, support vector machines (SVMs), and Gaussian process analysis, are examined to provide a comprehensive analysis of the data and improve forecasting accuracy.

Previous research efforts have focused on enhancing forecasts of pavement deformation and fractures through weather-specific adjustments. However, in this study, situated within the uniform meteorological framework of the Seoul Metropolitan Government, we chose not to implement such modifications, capitalizing on the consistent environmental conditions present across the examined sites. Using both empirical and analytical approaches, the prior research aimed to develop a reliable technique for forecasting reflective cracking on specific expressways in Seoul. The empirical model concentrated on variables such as average temperature, precipitation, and traffic volume, while the analytical model included variables like maximum temperature, precipitation, and minimum relative humidity. Despite having a similar computational structure, these models examined different sets of independent factors [22].

The simulations were designed to help authorities plan maintenance and repair activities more efficiently by offering insights into the likelihood of reflective cracking development through regression modeling and variable normalization.

2.1.2. Predictive Model and Enhancements for Improved Accuracy

In order to anticipate the development of reflective cracking, this study presents a predictive model that combines separate variables and coefficients. The reflective cracking prediction amount (E) depends on a combination of independent factors and unknown coefficients ($\beta_0, \ldots, \beta_{45}$). The empirical forecasting approach employs factors like mean temperature, rainfall, maximum snowfall, maximum consecutive days with precipitation, and

traffic volume to predict reflective cracking, whereas the analytical framework incorporates the highest temperature, precipitation, and the amount of traffic. These variables are inputs and are standardized between −1 and 1, where a value of −1 denotes a low probability of reflective cracking development and a value of 1 indicates a higher probability. This model provides a methodical way to assess and control reflective cracking risk, which is crucial for improving pavement management and upkeep techniques. Equation (1) illustrates how the design of experiments (DOEs) method was used to create the regression model [22].

$$\begin{gathered} E = \beta_0 + \beta_{10}x_1 + \beta_{20}x_2 + \beta_{30}x_3 + \beta_{40}x_4 + \beta_{50}x_5 + \beta_{11}x_1^2 + \beta_{22}x_2^2 \\ +\beta_{33}x_3^2 + \beta_{44}x_4^2 + \beta_{55}x_5^2 + \beta_{12}x_1x_2 + \beta_{13}x_1x_3 + \beta_{14}x_1x_4 + \beta_{15}x_1x_5 \\ +\beta_{23}x_2x_3 + \beta_{24}x_2x_4 + \beta_{25}x_2x_5 + \beta_{34}x_3x_4 + \beta_{35}x_3x_5 + \beta_{45}x_4x_5 \end{gathered} \quad (1)$$

Here is a detailed explanation of the factors and coefficients:

- E: This represents the reflective cracking prediction amount, which is the dependent variable we attempt to estimate.
- β_0 to β_{45}: These are the coefficients of the independent variables in the predictive model. Each coefficient represents the contribution of the corresponding independent variable to the prediction of reflective cracking.
- x_1 to x_5: These are the independent variables used in the predictive model. Each variable represents a different environmental or exploitation factor that may influence the occurrence of reflective cracking. Here is a breakdown of what each variable represents:
    - x_1: Mean temperature;
    - x_2: Relative humidity;
    - x_3: Largest amount of fresh snowfall;
    - x_4: Precipitation days;
    - x_5: Traffic volume.

In the empirical forecasting approach, x_1 to x_5 are standardized among −1 and 1, where a value of −1 denotes a low probability of reflective cracking development and a value of 1 indicates a higher probability. Each method provides unique insights into the prediction model, and these factors are selected based on their possible impact on the occurrence of reflective cracking [22].

Although helpful for broad forecasts in Seoul, the prior predictive model has many drawbacks. Its forecasts may not be accurate outside of its limited range because it mostly uses local data. Its dependability is also in doubt because it is purely based on past data and has not been verified by actual forecasts. The model was tested for accuracy by comparing it with real data for regions such as Buk-bu Expressway. The comparison showed that the model's success rate declined over time, suggesting that it might only be trustworthy for information up until 2022.

This shows that additional elements that might influence the occurrence of reflective cracking, such as changes in policies, were not taken into consideration by the model. The current study intends to improve the model's accuracy by taking into account further elements and upgrading its database to solve these problems.

In general, the focus is on forecasting reflective crack occurrences, considering weather and traffic statistics. Data from the National Meteorological Service and the Seoul Traffic Information Center revealed that high temperatures, rainfall, snowfall, humidity, and traffic volume significantly affect reflective crack predictions. Using these factors, a model was developed and tested, with data normalized to minimize errors. The analysis also accounted for traffic volume's impact on road deterioration, despite regulations on large vehicles. Multiple regression analysis was then used to assess the relationship between these variables and monthly reflective crack.

2.1.3. Supervised Learning Methods for Machine Learning Forecasting

This investigation employed machine learning methods using supervised learning techniques, including decision and regression trees, multiple regression, support vector machines (SVMs) [30], and Gaussian process analysis [43]. These methods, which segment data according to optimization levels, were used to analyze data and forecast results. For example, multiple regression explains the link between independent (X) and dependent (Y) variables, while SVMs use hyperplanes to group variables into clusters. Regression and decision trees make decisions based on reducing uncertainty and maximizing purity [44]. Gaussian process regression uses kernel functions to estimate continuous dependent variables, representing the relationship between input and output variables.

Each method offers a unique perspective to forecasting, contributing to a comprehensive examination of the data. The connection between the variables in the independent group (X) and the dependent variable (Y) is described by the analysis technique known as multiple regression [30]. This relationship can be determined by calculating the matrix's determinant for the estimation of parameters, as indicated in Equation (2):

$$min \sum_{i=1}^{N} \hat{\varepsilon}_i^2 = \sum_{i=1}^{N} \left(Y_i - \hat{Y}_i\right)^2 = \sum_{i=1}^{N} \left[[Y_i] - \left[\hat{\beta}_i\right] [X_i]^T \right]^2$$
$$\hat{\beta} = (X'X)^{-1} X'Y \quad (2)$$

where $\hat{\varepsilon}$ stands for the residual sum of squares and N is the number of independent variables. Regression analysis was used to obtain the $\hat{\beta}$ value, which led to the prediction model.

2.2. Reflection Cracking Detection Model

The second goal of the project was to develop effective techniques for creating a deep learning framework that is adaptable to different environments. Compiling the image collection required taking pictures of various pavement surfaces and ambient lighting. Preliminary data analysis highlighted these variables' potentially significant effects on reflective cracking detection performance. Moreover, anchor boxes are frequently produced by traditional bounding box methodologies [45], which are often used for reflective cracking surveillance but may not be precise in measuring and evaluating the amount of reflective cracking. To address this, our work used state-of-the-art Image Segmentation techniques to accurately delineate the area of reflective cracking areas [37].

2.2.1. Data Collecting and Pre-Processing

For this study, a training set of data was collected from various sources, including websites, in-person surveys, and Google Street View, to capture a wide range of pavement and air quality situations. For quality control reasons, the gathered images showed a range of resolutions, usually from 360p to 720p, with careful attention paid to obtaining a well-balanced depiction across various meteorological situations, lighting circumstances, and traffic settings [46]. After that, these pictures were manually labeled using the MATLAB Image Labeler application [47]. Eight hundred pictures were carefully classified as "Reflective cracking" based on professional advice and earlier studies. Comprehensive and exhaustive coverage of the data was ensured by the dataset's painstaking organization in COCO format, which included full annotations and captions for every image [47].

2.2.2. Data Labeling

Under the direction of a Korean pavement assessment specialist, reflection crack layouts were sketched and transcribed into JSON archives. The 1280 photos in the dataset were labeled using MATLAB 2023b Image Labeler, with the categories of "Reflective cracking" separated evenly [47]. The COCO-formatted dataset contains bounding polygon labels and comprehensive picture specs.

Table 1 presents a breakdown of the dataset used for training, validation, and testing in the context of pavement damage analysis. It categorizes the data by pavement types and weather conditions, indicating the number of samples allocated for each combination. For asphalt pavement, both clear and multiple weather scenarios were considered, with 256 samples each for training, 32 for validation, and 32 for testing, totaling 320 samples per condition. Similarly, concrete pavement data follows the same distribution, resulting in a total dataset size of 1280 samples [48]. This structured dataset ensures comprehensive coverage across various conditions, facilitating robust model development and evaluation for pavement damage detection.

Table 1. Overview of the composition of the dataset (number of images).

Pavement Types	Weather Types	Train Data	Validation Data	Test Data	Total
Asphalt pavement	Clear	256	32	32	320
	Multiple weather	256	32	32	320
Concrete pavement	Clear	256	32	32	320
	Multiple weather	256	32	32	320
Total		1024	128	128	1280

2.2.3. Data Augmentation

Image Data Generator enhanced photos to increase the diversity of the collection and make up for the lack of high-quality reflective cracking examples. Techniques included color upgrades (contrast, saturation) as well as positioning changes (flipping, scaling, and rotating) [16,49,50]. Processing was expedited by standardizing photos to 300 × 300 pixels and enlarging them from 200 to 600 pixels. To avoid over-augmentation for efficient model convergence, the dataset was divided into two halves: 80% for training and 20% for testing. This guided the creation of the model with the suggested architecture.

2.2.4. Deep Learning-Driven Object Identification

As shown in Figure 1, the automated reflection cracking segment was made possible by the modified Mask R-CNN design. This version of Mask R-CNN was specifically designed to enhance the recognition of reflective cracking, and it was trained using labeled photos [47]. Modeling creation was made simpler by using Detectron2, a modern object identification technique, which removed the need for a new Mask R-CNN network. Quick image segmentation was made possible by utilizing the Detectron2's pre-trained model, which facilitated transfer learning for object recognition in a variety of domains. Furthermore, three convolutional blocks and max pooling layers from the Keras deep learning framework were smoothly included in the sequential network.

2.2.5. Mask R-CNN

By adding object masks to bounding boxes, Mask R-CNN—a Faster R-CNN extension—improves the identification and segmentation of objects efficiency as shown in Figure 2. Pixel-level segmentation is made possible by RoIAlign, which guarantees accurate spatial features in region-of-interest pooling [51]. The Mask head comes next. The already trained models from Detectron2 were mainly employed in their default setups, with some hyperparameter value alterations [36]. In Mask R-CNN, models such as R101-FPN perform better than others, despite longer training times and the occasional excessive fitting issue.

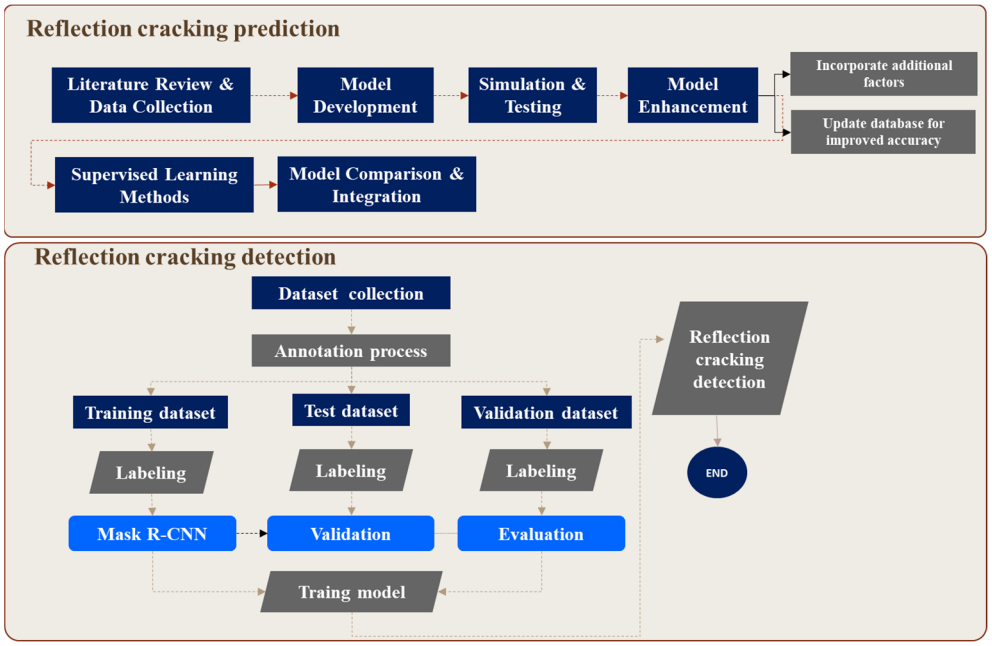

Figure 1. Framework for reflection cracking prediction and detection.

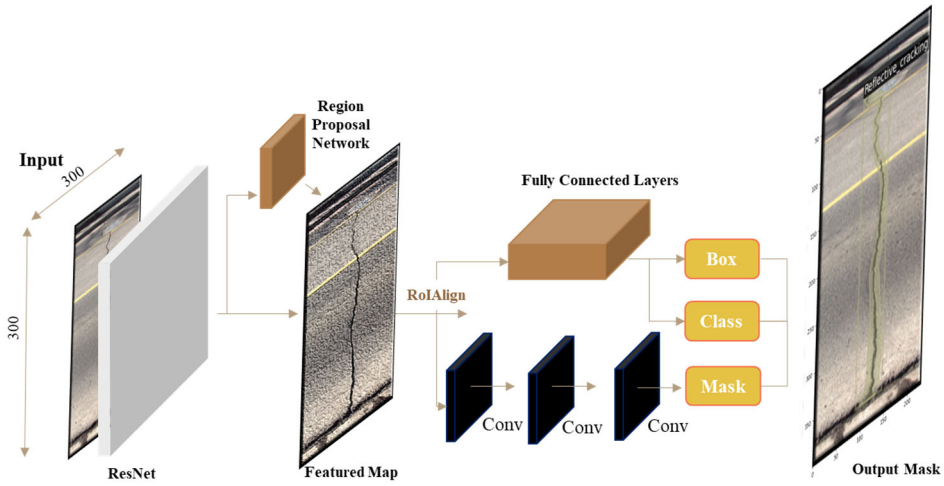

Figure 2. Mask R-CNN structure.

2.2.6. Applications

The main programming language used in this study was Python, and Google Colab provided the GPU environment—a Nvidia Tesla P100/K80/T4—for the development of all deep learning systems [52]. The popular data-flow computing and neural network creation tools TensorFlow and Keras were used to create the Mask R-CNN approach to reflective cracking identification. A model that was trained from the Common Objects in Context (COCO) database modified to fit the reflective cracking database was used for training.

2.2.7. Hyperparameters

After network topologies and datasets are finalized, it is imperative to set network hyperparameters before training. These parameters were found via heuristics as opposed to direct dataset estimates because they are not dependent on any particular dataset [48]. Although Mask R-CNN provides a wide range of hyperparameters to be adjusted during training, it can take a lot of time and resources to explore every possible configuration. Because of this, class numbers in the current study were designated as reflective cracking zones, and default settings were mostly employed. The default settings from Detectron2

were kept, while the parameters of the model, such as the learning algorithm, were adjusted using Optuna, a hyperparameter tuning tool [48].

Table 2 outlines the key hyperparameters for Mask R-CNN, crucial for its performance. These include a base learning rate of 0.00027, five images per batch, a gamma value of 0.06 for learning rate adjustment, and a maximum of 2000 iterations [47]. It also specifies 18 regions of interest per image and handles three distinct classes. Additionally, parameter cfg.MODEL.ROI_HEADS.SCORE_THRESH_TEST is set at 0.6 to balance recall and precision during evaluation. These settings collectively ensure the model's robustness and effectiveness across various computer vision tasks [47].

Table 2. Mask R-CNN hyperparameter setting.

Model Parameter	Value
cfg.SOLVER.BASE_LR	0.00027
cfg.SOLVER.IMS_PER_BATCH	5
cfg.SOLVER.GAMMA	0.06
cfg.SOLVER.MAX_ITER	2000
cfg.MODEL.ROI_HEADS.BATCH_SIZE_PER_IMAGE	18
cfg.MODEL.ROI_HEADS.NUM_CLASSES	3
cfg.MODEL.ROI_HEADS.SCORE_THRESH_TEST	0.6

2.2.8. Comparable Architectures

The most recent version of Ultralytics' YOLO V8 significantly increases object detection tasks' speed and accuracy [53]. Its integrated framework supports tasks like picture categorization and instance segmentation, while its rebuilt backbone network and an-chor-free head refine detecting powers. It provides models that have been trained with the recognition of object stages and is flexible in terms of export forms and CPU/GPU compatibility. YOLO V8, which comes in detection, segmentation, and classification variations, is a reliable choice that has gained recognition for its contributions to artificial recognition [53].

The authors of this study used a Kaggle dataset of 1280 reflective cracking photos, and they used the Pascal VOC annotation format to accurately pinpoint the reflective cracking spots in the photos. The dataset's separation into training and testing sets and intricacy were overcome by converting it into COCO format to satisfy the YOLOV8 model's needs. After preprocessing and splitting, the efficacy of the YOLOV8 framework for identifying reflective cracking forecasts was assessed during training. Improving the efficiency of models and guaranteeing correct object detection was made possible by data annotation with the help of tools such as RoboFlow. A crucial method that also became apparent was data augmentation, which improved the model's robustness versus changes in source data and enhanced the training dataset, increasing its precision and dependability in real-world projections.

Table 3 presents a comparative analysis of hyperparameter configurations across several notable architectures in the realm of object detection. The Yolov4 model [31], with an input size of 300 × 300, utilizes a momentum of 0.9 alongside a decay rate of 0.00005 and a learning rate of 0.0013, employing Leaky ReLU activation. In contrast, Yolov5 adopts a larger input dimension of 416 × 416, maintaining a momentum of 0.9 [38], a slightly higher decay of 0.0005, and a learning rate of 0.001, employing the ReLU activation function. Lastly, Yolov8 [53], also with a size of 416 × 416, employs a momentum of 0.85, a decay rate of 0.0003, and a learning rate of 0.002, utilizing the Mish activation function. These distinct configurations highlight the nuanced choices made in adjusting hyperparameters, catering to the specific requirements and architectural intricacies of each model, ultimately impacting their performance in object detection tasks.

Table 3. Hyperparameter configuration of comparable architectures.

Model	Width × Height	Momentum	Decay	Learning Rate	Activation
Yolov4	300 × 300	0.9	0.00005	0.0013	Leaky ReLU
Yolov5	416 × 416	0.9	0.0005	0.001	ReLU
Yolov8	416 × 416	0.85	0.0003	0.002	Mish

2.2.9. Comparative Analysis and Evaluation

Using a method that takes into account multiple parameters, an in-depth comparison was carried out to assess segmentation algorithms based on pixel recognition precision. Global accuracy (GA) is computed using an assessment method that includes true positives (TPs), true negatives (TNs), false positives (FPs), and false negatives (FNs). In order to additionally improve the segmentation framework, accuracy and Intersection-over-Union (IoU) scores were combined. IoU quantifies the overlap across predicted and reality segments [47]. Accuracy was ensured by establishing standards: a class was considered existent only if the final result possibility was more than 0.5, and true detection necessitated comparing the indicated bounding box with real data and requiring an IoU score of at least 50% [35]. This all-encompassing strategy made it possible to evaluate segmentation methods in depth, which helped with accurate choices on model improvement.

The following Equations (3) and (4) describe a comparison analysis conducted using the proportion of properly recognized pixels:

$$\mathrm{GA} = \frac{\mathrm{TP} + \mathrm{TN}}{\mathrm{TP} + \mathrm{TN} + \mathrm{FP} + \mathrm{FN}} \tag{3}$$

$$\mathrm{IoU} = \frac{\mathrm{TP}}{\mathrm{TP} + \mathrm{FP} + \mathrm{FN}} \tag{4}$$

2.2.10. Cross-Entropy Loss Function

The initial use of the traditional cross-entropy loss function (Equation (5)) in this study treats background and reflective cracking pixels equitably. However, this approach may not be the best choice for datasets including instances of uneven reflective cracking. To address this problem, a weighted binary cross-entropy loss function was devised, which is represented by Equation (6), where various weights are allocated to different types of pixels [54,55].

The traditional binary cross-entropy loss function is defined as follows:

$$\mathrm{L}(\mathrm{y}, \hat{y}) = -[\mathrm{y}\log(\hat{y}\,) + (1 - \mathrm{y})\log(1 - \hat{y})], \tag{5}$$

where

- y is the true label (0 for background, 1 for reflective cracking);
- $\hat{y}$ is the predicted probability;
- log denotes the natural logarithm.

To account for the uneven distribution of background and reflective cracking pixels, a weighted binary cross-entropy loss function is introduced. The weighted loss function is defined as

$$\mathrm{L}(\mathrm{y}, \hat{y}) = -[w_1 y \log(\hat{y}) + w_2(1 - y)\log(1 - \hat{y})], \tag{6}$$

where

- y is the true label (0 for background, 1 for reflective cracking);
- $\hat{y}$ is the predicted probability;
- w_1 is the weight assigned to the reflective cracking pixels;
- w_2 is the weight assigned to the background pixels;

- log denotes the natural logarithm.

By assigning different weights w_1 and w_2 to the different types of pixels, this weighted loss function better accommodates the uneven distribution in the dataset, improving the model's performance in identifying reflective cracking.

3. Results and Discussions

3.1. Reflection Cracking Prediction Results

3.1.1. Initial Multilinear Regression Analysis

Table 4 outlines the findings of multilinear regression analysis. It shows a strong correlation (R = 0.858) and a reasonable coefficient of determination (R^2 = 0.731). The Root Mean Squared Error (RMSE) is 1795.00, indicating the average deviation between observed and predicted values. The Mean Percentage Error (MPE) is 30.60%, suggesting overall accuracy.

Table 4. Result of multilinear regression analysis.

Model	R	R2	RMSE	MPE (%)	Std. Error of the Estimate
Regression Equation	0.858	0.731	1795.00	30.60	845.00

Table 5 uses multiple linear regression and correlation analysis to illustrate how different factors affect the prediction of reflective cracking. Both analyses highlight the strong positive relationships between reflective cracking frequency and traffic volume and precipitation, as well as the significant positive influence of the lowest temperature. The correlation and regression studies indicate that the maximum continuous precipitation day and average temperature are positively correlated with the occurrence of reflective cracking.

Table 5. Correlation Analysis Results for Predictive Factors in Pavement Damage.

Rank	Correlation Analysis	Multi-Linear Regression Analysis
	Correlation Factor	*p*-Value
1	Precipitation	0.612
2	Traffic Volume	0.550
3	Min. Temperature	0.510
4	Max. Continuous Precipitation Day	0.505
5	Avg. Temperature	0.502
6	Precipitation Day	0.446
7	Max. Snowfall	0.420
8	Max. New Snowfall	0.382
9	Relative Humidity	0.369
10	Min. Relative Humidity	0.317
11	Max. Temperature	0.192
12	Evaporation Loss	0.081

Additionally, there are further positive relationships between reflective cracking occurrence and variables such as maximum snowfall, maximum day of precipitation, and maximum amount of fresh snowfall. Regression analysis also supports the moderate positive associations between reflective cracking occurrence and minimum relative humidity, as well as the weaker positive relationships between evaporation loss and maximum temperature and reflective cracking occurrence. Overall, temperature-related factors, traffic volume, and precipitation appear to be the main determinants of the likelihood of reflective cracking.

According to the multilinear regression analysis, the key predictors for reflective cracking are monthly minimum temperature, traffic volume, total precipitation, highest

consecutive days with precipitation, and average temperature. Each of these variables has a significant correlation of 50% or more. The monthly minimum and average temperatures, relative humidity, and precipitation appear to be independent in terms of collinearity among the independent variables. Additionally, a distinct group is formed by the lowest relative humidity, the greatest number of consecutive days with precipitation, and the maximum depth of newly fallen snow.

The lowest temperature has the highest correlation with the occurrence of reflective cracking, followed by relative humidity, precipitation, and traffic volume, as indicated by the standardization coefficient ranking. Despite its strong link with reflective cracking, minimum relative humidity is not selected because it overlaps with other variables. Instead, the ultimate independent factors chosen are the greatest number of consecutive days with rainfall and the maximum depth of newly fallen snow.

3.1.2. Comparison of Machine Learning Techniques for Model Optimization

Machine learning techniques were applied to optimize both empirical and analytical models, aiming to minimize errors using RMSE, MSE, and MAE (Table 6). Training velocity and time were also evaluated. The multilinear regression model emerged as the optimal choice due to its minimal error, while stepwise regression, despite its fast training speed, exhibited lower prediction efficiency and larger margins of error.

Table 6. Machine learning yielded optimization results.

Model	Metric	NH19 Empirical	NH19 Analytical	NH23 Empirical	NH23 Analytical
Linear Regression	RMSE	0.278	0.295	0.238	0.248
	MSE	0.077	0.087	0.057	0.062
	MAE	0.195	0.198	0.164	0.184
	T.V (n/s)	2000	2100	2100	1800
	T.T (s)	1.467	1.563	1.476	1.524
Stepwise Linear Reg.	RMSE	4.737	0.948	2.815	0.496
	MSE	22.439	0.898	7.923	0.246
	MAE	1.115	0.583	0.926	0.383
	T.V (n/s)	3100	2900	2800	3000
	T.T (s)	101.97	110.48	113.97	114.96
Decision Tree	RMSE	0.413	0.429	0.432	0.353
	MSE	0.171	0.184	0.186	0.125
	MAE	0.298	0.323	0.318	0.244
	T.V (n/s)	4300	3600	3200	3800
	T.T (s)	0.81	1.016	0.876	0.938
Support Vector Machine	RMSE	0.368	0.359	0.334	0.331
	MSE	0.136	0.129	0.112	0.109
	MAE	0.248	0.241	0.229	0.231
	T.V (n/s)	4400	3600	4700	3700
	T.T (s)	0.414	0.609	0.476	0.568

Table 6. *Cont.*

Model	Metric	NH19 Empirical	NH19 Analytical	NH23 Empirical	NH23 Analytical
Ensemble	RMSE	0.379	0.405	0.365	0.325
	MSE	0.144	0.164	0.133	0.106
	MAE	0.257	0.297	0.268	0.227
	T.V (n/s)	1400	1300	1400	1600
	T.T (s)	1.532	1.8	1.45	1.34
Gaussian Process Reg.	RMSE	0.406	0.383	0.343	0.317
	MSE	0.165	0.146	0.118	0.1
	MAE	0.28	0.263	0.252	0.214
	T.V (n/s)	3500	2100	3500	1500
	T.T (s)	0.797	1.676	0.441	0.465

Root Mean Squared Error (RMSE); Mean Squared Error (MSE); Mean Absolute Error (MAE); Traffic volume (T.V); Travel time (T.T).

The optimized multilinear regression model underwent coefficient adjustments based on previous studies, and the updated variables of Equation (1) are presented in Table 7. Using these refined coefficients, occurrences of reflective cracking were predicted. Figure 3 illustrates the comparison between actual and predicted values, showcasing the improved performance of the new predictive model, which integrates weather, traffic volume, and reflective cracking survey data from 2022. Standardization of variables was crucial to enhance accuracy, especially given the diverse ranges in traffic and temperature.

Table 7. Determination of regression coefficients.

	Empirical Approach		Analytical Approach	
	NH19 Roadway	NH23 Expressway	NH19 Roadway	NH23 Expressway
R^2	0.686	0.803	0.635	0.783
MSE	0.077	0.057	0.087	0.062
MAE	0.195	0.164	0.198	0.184
β_0	−1.363	−2.571	−1.043	1.365
β_{10}	2.328	2.102	0.744	−0.427
β_{20}	−3.154	−0.711	−0.813	0.608
β_{30}	0.001	−3.793	−0.491	−0.437
β_{40}	1.128	−0.271	−0.420	2.439
β_{50}	0.473	−1.635	−1.000	3.224
β_{11}	0.311	0.197	−0.212	0.079
β_{22}	−1.855	1.258	0.306	−2.471
β_{33}	0.862	−0.728	−0.247	0.327
β_{44}	−0.537	0.336	0.151	−0.667
β_{55}	0.285	0.546	0.162	−0.363
β_{12}	1.271	−0.815	0.389	−0.633
β_{13}	1.696	0.929	0.995	0.050
β_{14}	−0.499	−0.465	−0.426	0.235
β_{15}	−0.100	1.542	−0.007	0.143
β_{23}	−1.857	−0.627	−1.380	−0.696
β_{24}	1.878	0.856	0.128	3.515
β_{25}	0.571	−0.962	0.010	4.274
β_{34}	0.155	0.053	0.130	0.412
β_{35}	−0.015	−3.320	−1.132	−0.182
β_{45}	0.133	−0.521	−0.391	−0.218

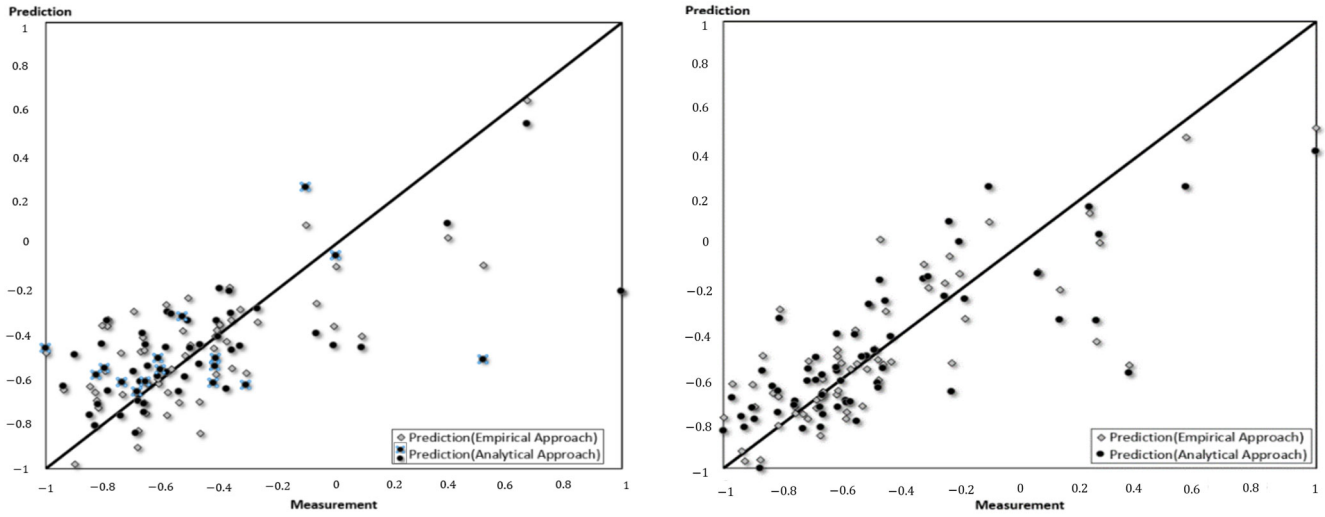

Figure 3. The numbers of predicted reflective cracking: (**a**) NH19 Roadway and (**b**) NH23 Expressway.

Further evaluation involved a comparative analysis between analytical and empirical approaches, with the predictive model's efficacy confirmed by forecasting reflective cracking numbers for 2022, a period not included in the initial training or verification phase.

Figure 4 illustrates the performance of the prediction model based on actual reflective cracking occurrences, utilizing standardized values ranging from −1 to 1.

Figure 4a displays the prediction outcomes from the NH19 roadway area, whereas Figure 4b showcases the prediction outcomes from the NH23 roadway area. This finding presents the performance evaluation of the developed prediction models, with the empirical method showing proper performance, particularly on NH19 and NH23 expressways. Given its efficiency across locations, the empirical approach is recommended for standardized reflective cracking prediction in pavement management systems. Additionally, the recalibrated model can aid in cost analysis by accurately predicting reflective cracking occurrences, facilitating optimal budget allocation, and preventing budgetary discrepancies.

Furthermore, Table 8 provides a comprehensive assessment of the developed prediction models, considering both the standardization method and the methodologies used (empirical versus analytical). The performance metrics evaluated include Root Mean Squared Error (RMSE), Mean Absolute Error (MAE), Mean Squared Error (MSE), coefficient of determination (R^2), and the *p*-value.

Table 8. Assessment of the effectiveness of developed prediction models.

	Standardization									
	Empirical Approach					Analytical Approach				
	RMSE	MAE	MSE	R^2	*p*-Value	RMSE	MAE	MSE	R^2	*p*-Value
NH19	0.5355	0.4217	0.2867	0.5612	5.81×10^{-6}	0.5743	0.4182	0.3299	0.7151	0.0003
NH23	0.6138	0.4549	0.3767	0.4314	0.4548	0.5691	0.4619	0.3239	0.4302	9.68×10^{-10}
	Reflective cracking Prediction									
	Empirical Approach					Analytical Approach				
	RMSE	MAE	MSE	R^2	*p*-Value	RMSE	MAE	MSE	R^2	*p*-Value
NH19	344	272	118,598	0.5613	0.2495	369	269	136,390	0.7148	0.0869
NH23	490	363	239,995	0.4314	0.0231	454	369	206,142	0.4303	0.0040

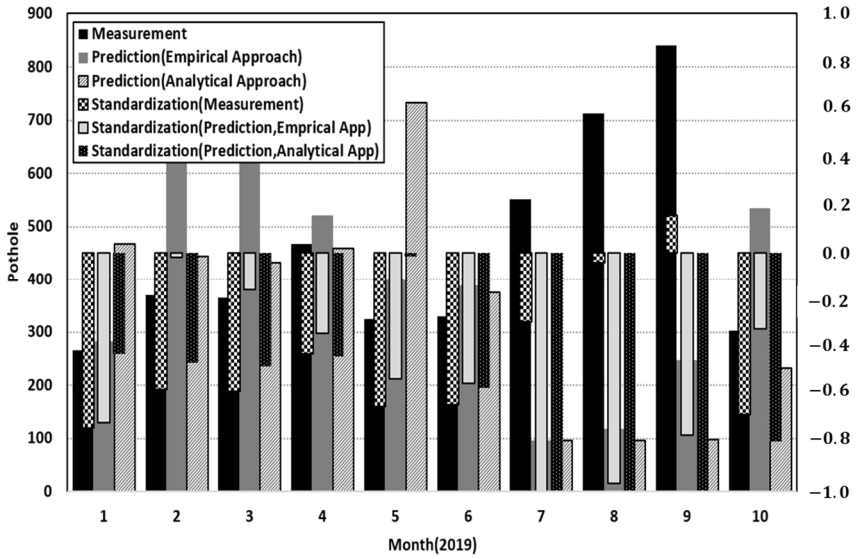

(**a**)

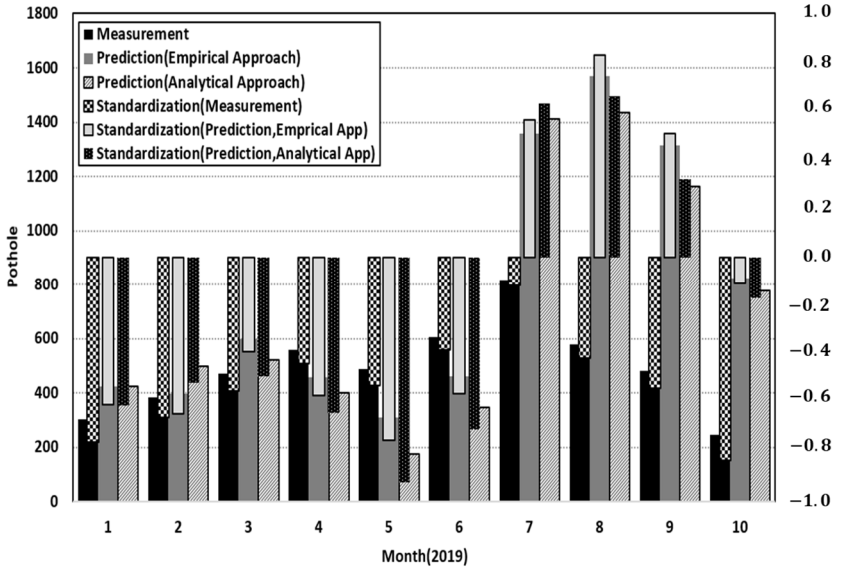

(**b**)

Figure 4. Assessment of predictive model performance for NH19 and NH23. (**a**) Prediction results from NH19 roadway zone. (**b**) Prediction results from NH23 roadway zone.

For the NH19 district, both empirical and analytical approaches demonstrate competitive results, with slight variations observed in RMSE, MAE, and MSE values. However, the R^2 values indicate better explanatory power for the analytical approach, suggesting a stronger fit to the data. The corresponding *p*-values underscore the statistical significance of the models, further validating their reliability.

Similarly, for the NH23 district, both approaches yield comparable results in terms of RMSE, MAE, and MSE. However, the analytical approach exhibits higher R^2 values, indicating superior predictive performance. Additionally, the significantly low *p*-values emphasize the statistical significance of the analytical model in capturing the underlying patterns of reflective cracking occurrence.

In summary, both empirical and analytical approaches demonstrate promising performance in predicting reflective cracking in the NH19 and NH23 districts. However, the analytical approach appears to offer slightly better predictive accuracy and statistical significance, particularly evident in the R^2 values and *p*-values. These findings highlight the

importance of considering both methodological approaches and standardization techniques in developing robust predictive models for reflective cracking.

3.1.3. Limitations

Although our finding has provided valuable insights into predictive modeling for pavement reflective cracking using multilinear regression, it is important to acknowledge its limitations. One notable limitation is the exclusive reliance on polynomial functions within the regression model, neglecting the potential benefits of non-polynomial functions. Non-polynomial functions, particularly in the context of mechanics of cracked media, offer a more nuanced representation of complex phenomena, including possible singularities that may arise in pavement degradation processes. Therefore, in the next stage of the research, the aim is to address this limitation by considering non-polynomial functions and leveraging insights from this method [56]. This expansion of modeling techniques will enable a more comprehensive understanding of reflective cracking mechanisms and pave the way for enhanced predictive accuracy and robustness in pavement management practices.

3.2. Reflective Cracking Categorization

Table 9 presents the average precision scores obtained from different types of datasets for reflective cracking categorization. Two machine learning methods, including image classification, were employed across various pavement types to assess their precision rates under distinct conditions. For concrete pavement, image classification achieved an average precision of 95.9% under clear weather conditions and 91.4% under multiple weather scenarios. Similarly, for asphalt pavement, the average precision was recorded at 92.7% under clear weather conditions and 82.6% under multiple weather conditions. These precision scores provide insights into the effectiveness of image classification techniques in accurately categorizing reflective cracking across different pavement types and weather conditions.

Table 9. The accuracy results of reflective cracking categorization.

No.	Machine Learning Methods	Pavement Types	Precision Clear (%)	Multiple Weather (%)
1	Image classification	Concrete pavement	95.9	91.4
2	Image classification	Asphalt pavement	92.7	82.6

In concrete pavement, the detection effectiveness of reflective cracking is typically better due to several factors. One key reason is the stark contrast between the cracks and the concrete background. Cracks in concrete pavement often appear as dark lines against a light or white background, making them easier to detect using image processing techniques. The high contrast between the cracks and the background facilitates the segmentation of cracks from the surrounding pavement surface, leading to more accurate detection.

Additionally, concrete pavement tends to have a smoother surface texture compared to asphalt pavement, which can further aid in the detection process. The relatively uniform texture of concrete makes it easier to distinguish cracks from other surface irregularities, reducing the likelihood of false positives in the detection results. Moreover, concrete pavement is often characterized by its durability and resistance to deformation, which can result in more distinct and well-defined cracks compared to asphalt pavement. These well-defined cracks provide clearer visual cues for automated detection algorithms, improving the overall effectiveness of crack detection systems.

3.3. Reflective Cracking Segmentations

3.3.1. Overall Results

The results validate the effectiveness of detecting reflective cracking on roadways using the Image Segmentation technique, as illustrated in Figure 5. The method developed

for detecting reflective cracking with Mask R-CNN performs satisfactorily, effectively differentiating between good pavement and reflective cracking pavement.

(**a**)

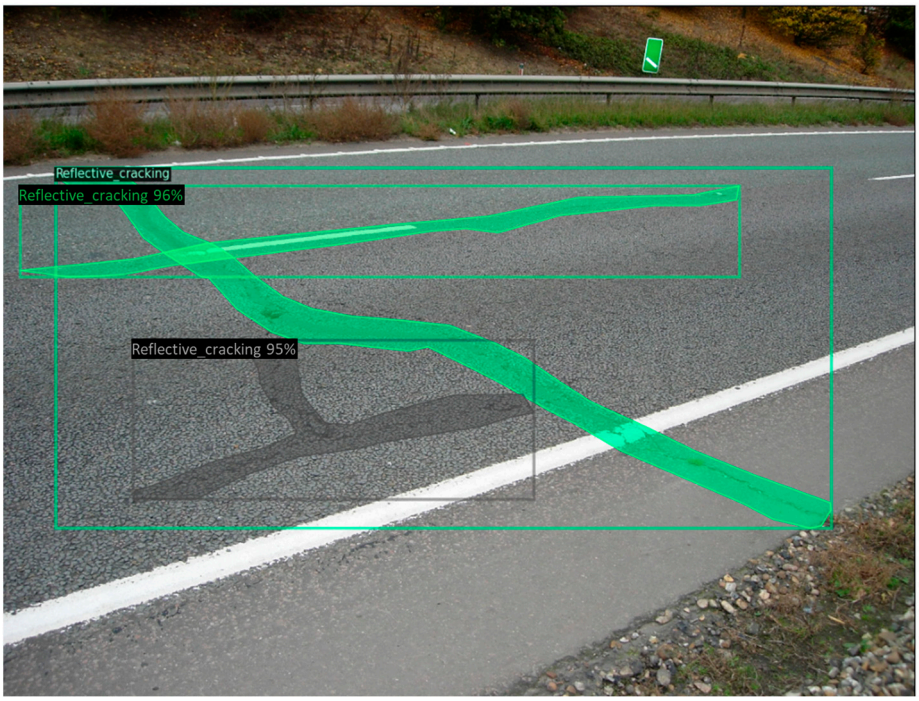

(**b**)

Figure 5. *Cont.*

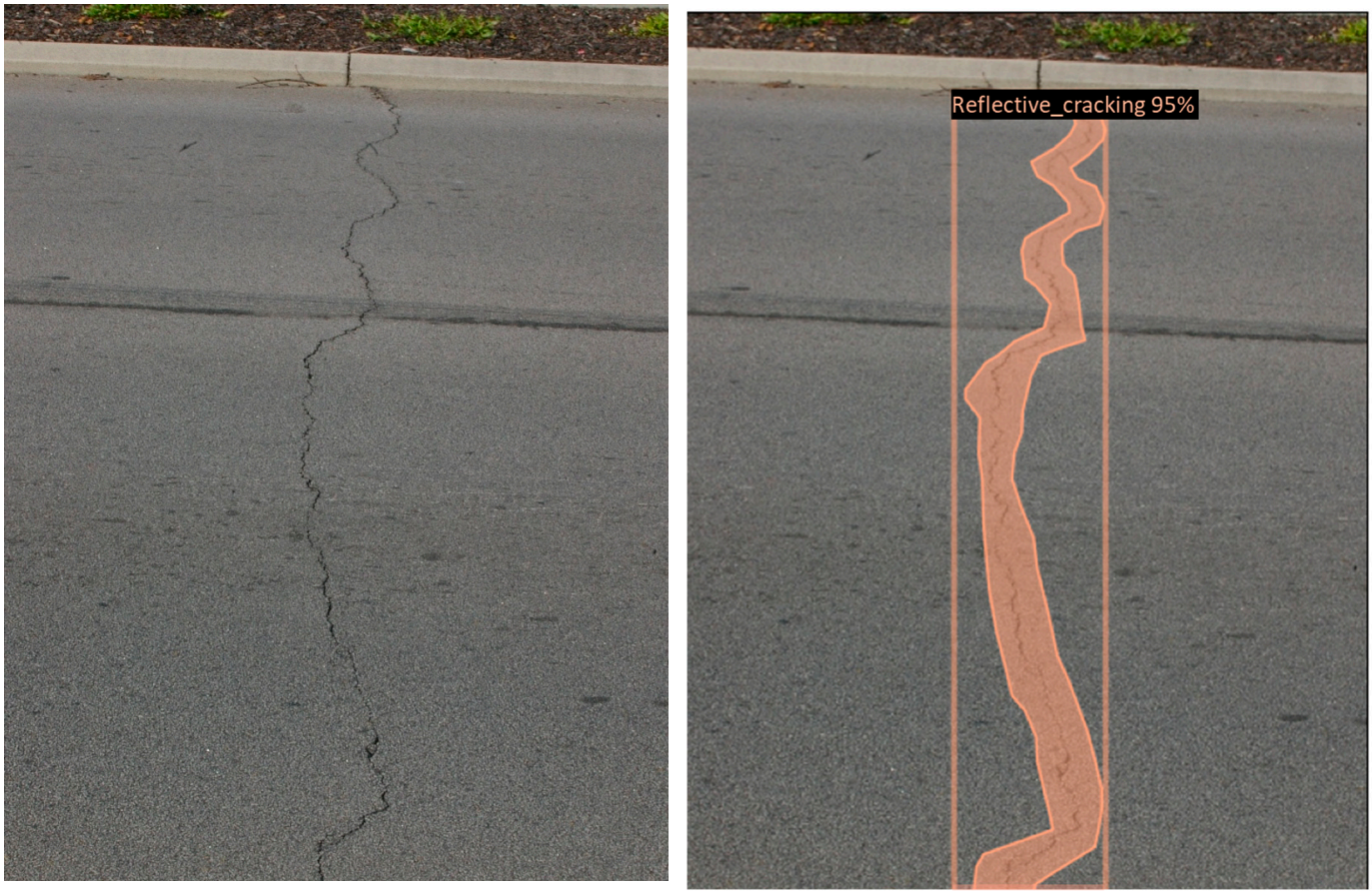

(**c**)

(**d**)

Figure 5. *Cont.*

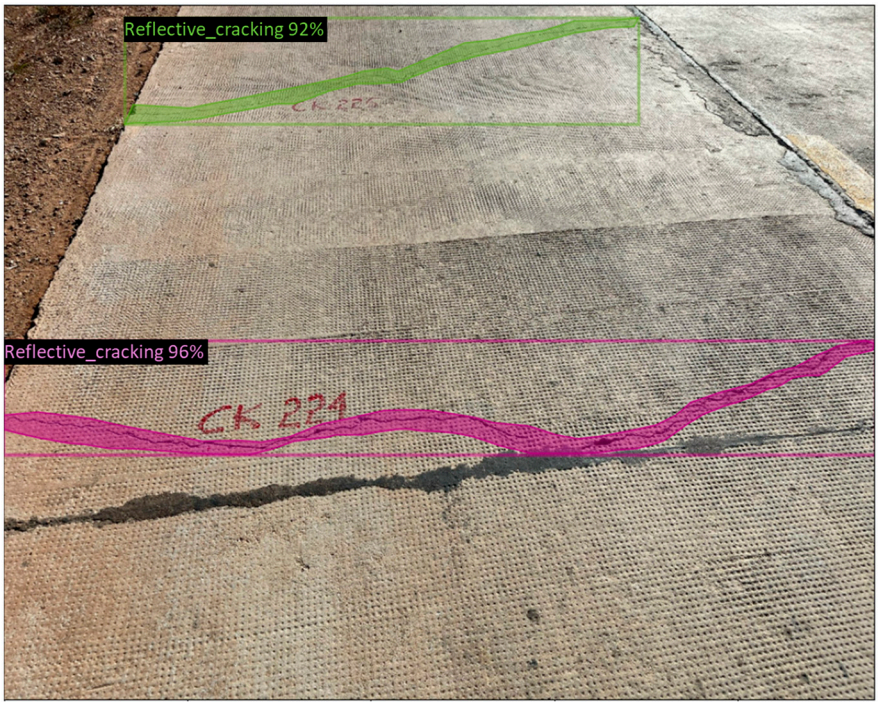

(**e**)

Figure 5. Results from the trained model for detecting reflective cracking. (**a**) Original photo of reflective cracking on urban road; (**b**) Classified photo of reflective cracking on urban road; (**c**) Original vs. classified photo of reflective cracking on a rural road; (**d**) Original photo of reflective cracking on concrete road; (**e**) Classified photo of reflective cracking on concrete road.

In the examples provided, the detection performance for reflective cracking is impressive on both types of pavements, with accuracy exceeding 90% in most cases. However, there is a notable distinction in detection effectiveness between concrete and asphalt pavements. On concrete pavement, the detection score approaches nearly 99%, showcasing a superior capability to accurately identify reflective cracks. Conversely, on asphalt pavement, both in rural and urban settings, the detection rates hover around 96%, indicating a slightly lower but still commendable performance. This discrepancy suggests that while detection remains highly effective on both pavement types, the inherent characteristics of concrete pavement, such as its smoother texture and the high contrast between cracks and the surface, contribute to its exceptional detection capabilities.

3.3.2. Weather Impact on Training Efficiency

Training scenarios involving loss and precision in relation to various climate variables are illustrated in Figure 6. Overall, the proposed model for reflective cracking detection demonstrates satisfactory efficiency indicators. As a detection approach, Mask R-CNN performs well, consistently achieving a total loss of less than 0.3 and a precision greater than 0.9. Convergence typically occurs after 2000 iterations, except for databases containing diverse meteorological conditions, which require additional training up to 4000 iterations.

The impact of climate information on training effectiveness is significant; introducing multiple meteorological photographs is particularly impactful, with larger databases correlating with lower results. This outcome highlights the negative effect of varied weather conditions on accuracy, aligning with other findings in image classification. The performance variance between datasets containing only clear weather photographs and those with all meteorological types underscores the crucial role that climate parameters play in successful training. This can be attributed to the similar characteristics of reflective cracking and other surface irregularities, especially in cloudy and rainy weather.

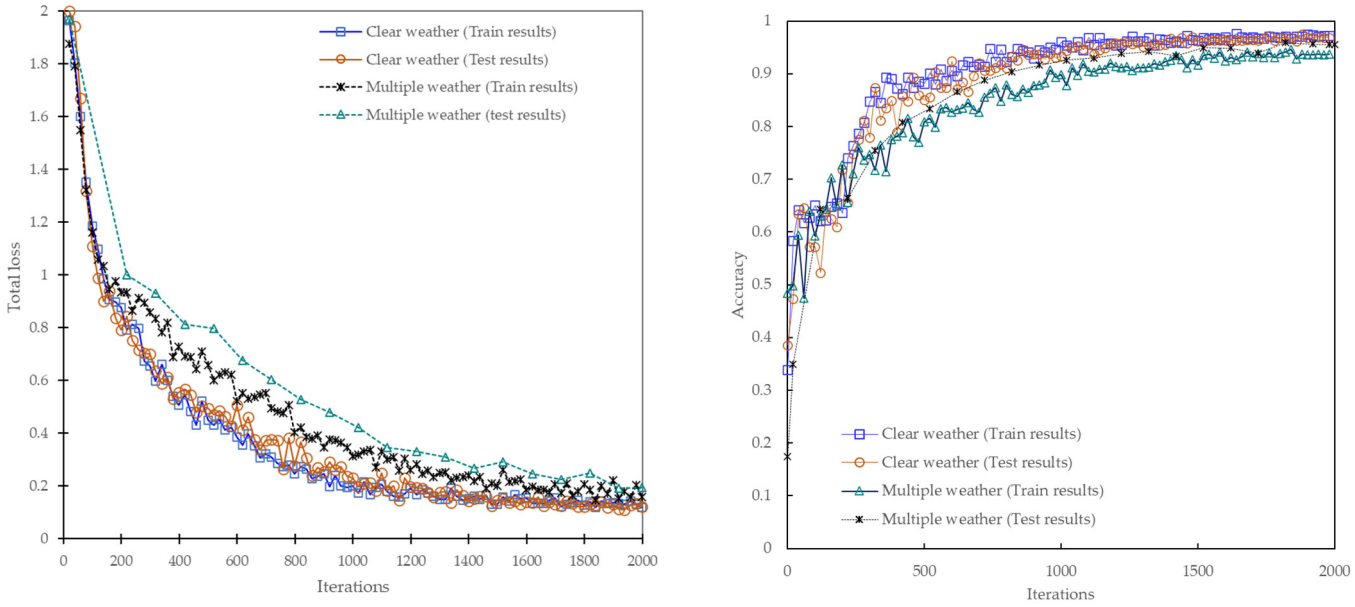

(**a**) (**b**)

Figure 6. Bounding box-based object identification method training outcomes are shown as (**a**) Total loss versus Iterations and (**b**) Mask-RCNN accuracy versus Iterations.

The model's efficacy is validated by the test dataset evaluation, with all testing groups achieving an accuracy of more than 80% using Mask R-CNN. Despite a slight discrepancy in performance between the training and test datasets—possibly due to fluctuations in surrounding conditions—the model performs consistently in all circumstances.

Even with a few small errors, the results support the applicability of this method for computerized reflective cracking assessment on roads. There were times when overestimations of reflective cracking severity occurred, especially in the identification of climatic conditions. Expanding the quantity of the training dataset may improve the classifier's accuracy and flexibility for future uses. In addition, a comprehensive analysis of the model's parameters was carried out to maximize performance. Using a mini-batch size of four, the loss function was minimized iteratively throughout learning in order to guarantee thorough convergence and avoid excessive fitting. The learning rate of 0.00025, the momentum of 0.8, the regularization of 0.0001, and the mini-batch size of 4 are the optimum model parameters.

3.3.3. Results of Average Precision at 50%

Table 10 provides an overview of the segmentation accuracy used to identify reflective cracking. The findings show that, out of the two categories, the second circumstance has the least accuracy, while the "Clear settings" have the most reliability. For example, the mean accuracy for the first and second circumstances is 92.5% and 83.7%, respectively, for IOU = 0.5 (AP50). These results imply that different contexts may have an effect on reflective cracking identification by picture segmentation. Furthermore, the incorporation of concrete pavement brings uncertainty to the accuracy of the model.

Since the segmentation may mistakenly see reflected cracking as a pattern on the pavement surface, the "black" color of asphalt pavement could lead to errors throughout training. Once reflective cracking occurs throughout the training period, it could be mistaken for the black pattern on the road surface. These findings demonstrate how difficult it can be to recognize reflective cracking in practical environments.

Table 10. AP50 results.

No.	Pavement Types	AP50: the Average Precision at IOU = 0.5	
		Combined Weather Data	
		1st Cond. Clear	2nd Cond. Multiple Weathers
1	Concrete pavement	92.5%	83.7%
2	Asphalt pavement and Concrete pavement	89.1%	80.3%

3.4. Architecture Comparison

Table 11 provides a comprehensive comparison of performance metrics across multiple architectures utilized for the pavement damage detection task. The evaluated architectures include Mask R-CNN, Yolov8, Yolov5, and Yolov4. Notably, the table showcases the time required per iteration for each architecture, with Mask R-CNN having a time of 0.92 s, while Yolov8 demonstrates the most efficient performance with a reduced time requirement of 0.75 s. Furthermore, the table presents the average precision at 50% Intersection over Union (AP50) on clear weather conditions, specifically on asphalt pavement. Mask R-CNN achieves an impressive AP50 score of 92.5%, closely followed by Yolov8 with 91.3%. These findings underscore the efficiency and accuracy of different architectures in the context of pavement damage detection, offering valuable insights for practitioners and researchers in the field.

Table 11. Comparisons of performance across several architectures.

	Mask R-CNN	Yolov8	Yolov5	Yolov4
Time needed per iteration (in seconds)	0.92	0.75	0.81	0.87
AP50 on clear weather	92.5%	91.3%	87.8%	83.4%

3.5. Challenges in Implementation

During the experimental process of implementing the proposed method, several challenges surfaced, reflecting the complex nature of pavement management and reflective cracking detection. One significant obstacle pertained to the variability of environmental conditions and pavement types across different regions. The diverse weather patterns and road surface characteristics posed challenges in training and validating the models effectively. To address this, a rigorous approach to data collection was adopted, incorporating a wide range of weather data and pavement images from various sources. Additionally, fine-tuning the deep learning algorithms required iterative experimentation and parameter optimization to ensure robust performance across different scenarios. Moreover, the interpretability of the models and the potential biases in the training data presented ongoing challenges in achieving generalizability and reliability. To mitigate these issues, comprehensive sensitivity analyses and model validations were conducted, leveraging cross-validation techniques and external validation datasets where possible. Despite these challenges, the study underscores the importance of continuous refinement and validation of predictive models in real-world applications, paving the way for more accurate and reliable pavement management strategies in the future.

4. Conclusions

This study investigates predictive and detection methods for reflective cracking in pavement infrastructure, combining machine learning and advanced image detection techniques. By employing algorithms such as linear regression and Mask R-CNN, predictive models and precise detection methods were developed. These approaches aim to enhance pavement management systems by enabling automatic monitoring and assessment of pavement conditions, ultimately improving maintenance strategies.

- The refined multilinear regression model exhibited improved predictive performance for reflective cracking occurrences. By integrating data from weather, traffic volume, and reflective cracking surveys spanning 2014 to 2018, the model achieved heightened accuracy. Standardization of variables was crucial for accuracy enhancement, particularly given the diverse ranges in traffic and temperature. Comparative analysis between analytical and empirical approaches further validated the model's efficacy, as it successfully forecasted reflective cracking numbers for 2019, a period not included in its initial training.
- The comprehensive evaluation of prediction models highlights the competitive performance of both empirical and analytical approaches across the NH19 and NH23 districts. For the NH19 district, the empirical approach yielded RMSE, MAE, and MSE values of 0.5355, 0.4217, and 0.2867, respectively, while the analytical approach demonstrated slightly improved values of 0.5743, 0.4182, and 0.3299, indicating a stronger fit to the data.
- The findings highlight the effectiveness of image classification techniques in categorizing reflective cracking across various pavement types and weather conditions, as evidenced by precision rates derived from extensive datasets. Notably, for concrete pavement, image classification achieved remarkable precision rates of 95.9% under clear weather and 91.4% under various weather scenarios. Conversely, for asphalt pavement, slightly lower but still impressive average precision scores of 92.7% under clear weather and 82.6% under multiple weather conditions were attained. Concrete pavement's superior detection effectiveness can be attributed to several factors, including its high contrast with cracks against the background, smoother surface texture aiding segmentation, and durability leading to well-defined cracks.
- The Mask R-CNN model showed strong performance in detecting reflective cracking, maintaining a total loss below 0.3 and a precision above 0.9. While convergence typically happens after 2000 iterations, datasets with varied weather conditions may require up to 4000 iterations for optimal training. The impact of climate data on training is significant, with diverse weather conditions correlating with lower results. The model's effectiveness was validated by achieving over 80% accuracy in all testing scenarios, despite slight performance variations, indicating its reliability across different conditions.
- The AP50 results illustrate segmentation accuracy for reflective cracking identification, revealing varied reliability across contexts. "Clear settings" exhibited the highest reliability, while the "multiple weather" scenario displayed the least reliability. Mean accuracies for these conditions were 94.7% and 82.4%, respectively, for IOU = 0.5 (AP50). The integration of the "black" color of asphalt pavement poses challenges, potentially leading to mistaken identification. These findings underscore the practical difficulty in recognizing reflective cracking.
- Mask R-CNN and Yolov8 exhibited top performance in pavement damage detection, with AP50 scores of 92.5% and 91.3%, respectively, under clear weather conditions for asphalt pavement.

Author Contributions: S.-P.S. and T.H.M.L.: conceptualization, methodology, writing—original draft. K.K., S.-P.S. and T.H.M.L.: visualization, investigation, writing—review, and editing. S.-P.S. and T.H.M.L.: data curation, software. All authors have read and agreed to the published version of the manuscript.

Funding: This research received no external funding.

Data Availability Statement: The original contributions presented in the study are included in the article, further inquiries can be directed to the corresponding author.

Conflicts of Interest: The authors declare no conflicts of interest, financial or otherwise.

References

1. Dhakal, N.; Elseifi, M.A.; Zhang, Z. Mitigation Strategies for Reflection Cracking in Rehabilitated Pavements—A Synthesis. *Int. J. Pavement Res. Technol.* **2016**, *9*, 228–239. [CrossRef]
2. Tam, A.B.; Park, D.W.; Le, T.H.M.; Kim, J.S. Evaluation on Fatigue Cracking Resistance of Fiber Grid Reinforced Asphalt Concrete with Reflection Cracking Rate Computation. *Constr. Build. Mater.* **2020**, *239*, 117873. [CrossRef]
3. Fallah, S.; Khodaii, A. Reinforcing Overlay to Reduce Reflection Cracking; An Experimental Investigation. *Geotext. Geomembr.* **2015**, *43*, 216–227. [CrossRef]
4. Ji, R.Y.; Mandal, T.; Yin, H. Laboratory Characterization of Temperature Induced Reflection Cracks. *J. Traffic Transp. Eng.* **2020**, *7*, 668–677. [CrossRef]
5. Doh, Y.S.; Baek, S.H.; Kim, K.W. Estimation of Relative Performance of Reinforced Overlaid Asphalt Concretes against Reflection Cracking Due to Bending More Fracture. *Constr. Build. Mater.* **2009**, *23*, 1803–1807. [CrossRef]
6. Khodaii, A.; Fallah, S.; Moghadas Nejad, F. Effects of Geosynthetics on Reduction of Reflection Cracking in Asphalt Overlays. *Geotext. Geomembr.* **2009**, *27*, 1–8. [CrossRef]
7. Chen, Y.; Zhu, Z.; Lin, Z.; Zhou, Y. Building Surface Crack Detection Using Deep Learning Technology. *Buildings* **2023**, *13*, 1814. [CrossRef]
8. Xi, Y.F.; Ren, S.J.; Chen, B.L.; Yang, B.; Lee, J.; Zhu, G.H.; Zhou, T.C.; Xu, H. Application of Steel-Fiber-Reinforced Self-Stressing Concrete in Prefabricated Pavement Joints. *Buildings* **2023**, *13*, 2129. [CrossRef]
9. Lu, X.; Yan, G. A Quasi-2D Exploration of Mixed-Mode Fracture Propagation in Concrete Semi-Circular Chevron-Notched Disks. *Buildings* **2023**, *13*, 2633. [CrossRef]
10. Di Mascio, P.; Moretti, L. Implementation of a Pavement Management System for Maintenance and Rehabilitation of Airport Surfaces. *Case Stud. Constr. Mater.* **2019**, *11*, e00251. [CrossRef]
11. Zhao, Y.; Goulias, D.; Peterson, D. Recycled Asphalt Pavement Materials in Transport Pavement Infrastructure: Sustainability Analysis & Metrics. *Sustainability* **2021**, *13*, 8071. [CrossRef]
12. Moradi, M.; Assaf, G.J. Building an Augmented Reality Experience on Top of a Smart Pavement Management System. *Buildings* **2022**, *12*, 1915. [CrossRef]
13. Shu, X.; Wang, Z.; Basheer, I.A. Large-Scale Evaluation of Pavement Performance Models Utilizing Automated Pavement Condition Survey Data. *Int. J. Transp. Sci. Technol.* **2022**, *11*, 678–689. [CrossRef]
14. Justo-Silva, R.; Ferreira, A.; Flintsch, G. Review on Machine Learning Techniques for Developing Pavement Performance Prediction Models. *Sustainability* **2021**, *13*, 5248. [CrossRef]
15. Pei, L.; Sun, Z.; Xiao, L.; Li, W.; Sun, J.; Zhang, H. Virtual Generation of Pavement Crack Images Based on Improved Deep Convolutional Generative Adversarial Network. *Eng. Appl. Artif. Intell.* **2021**, *104*, 104376. [CrossRef]
16. Que, Y.; Dai, Y.; Ji, X.; Kwan Leung, A.; Chen, Z.; Tang, Y.; Jiang, Z. Automatic Classification of Asphalt Pavement Cracks Using a Novel Integrated Generative Adversarial Networks and Improved VGG Model. *Eng. Struct.* **2023**, *277*, 115406. [CrossRef]
17. Patel, T.; Guo, B.H.W.; van der Walt, J.D.; Zou, Y. Effective Motion Sensors and Deep Learning Techniques for Unmanned Ground Vehicle (UGV)-Based Automated Pavement Layer Change Detection in Road Construction. *Buildings* **2023**, *13*, 5. [CrossRef]
18. Tabatabai, H.; Aljuboori, M. A Novel Concrete-Based Sensor for Detection of Ice and Water on Roads and Bridges. *Sensors* **2017**, *17*, 2912. [CrossRef]
19. Rhee, J.Y.; Park, K.T.; Cho, J.W.; Lee, S.Y. A Study of the Application and the Limitations of Gpr Investigation on Underground Survey of the Korean Expressways. *Remote Sens.* **2021**, *13*, 1805. [CrossRef]
20. Ramanna, S.; Sengoz, C.; Kehler, S.; Pham, D. Near Real-Time Map Building with Multi-Class Image Set Labeling and Classification of Road Conditions Using Convolutional Neural Networks. *Appl. Artif. Intell.* **2021**, *35*, 803–833. [CrossRef]
21. Zhang, L.; Yang, F.; Daniel Zhang, Y.; Zhu, Y.J. Road Crack Detection Using Deep Convolutional Neural Network. In Proceedings of the 2016 IEEE International Conference on Image Processing—ICIP, Phoenix, AZ, USA, 25–28 September 2016; pp. 3708–3712. [CrossRef]
22. Lee, S.Y.; Le, T.H.M.; Kim, Y.M. Prediction and Detection of Potholes in Urban Roads: Machine Learning and Deep Learning Based Image Segmentation Approaches. *Dev. Built Environ.* **2023**, *13*, 100109. [CrossRef]
23. Dong, C.Z.; Catbas, F.N. A Review of Computer Vision–Based Structural Health Monitoring at Local and Global Levels. *Struct. Health Monit.* **2021**, *20*, 692–743. [CrossRef]
24. Harrou, F.; Zeroual, A.; Hittawe, M.M.; Sun, Y. Recurrent and Convolutional Neural Networks for Traffic Management. *Road Traffic Model. Manag.* **2022**, 197–246. [CrossRef]
25. Harrou, F.; Zeroual, A.; Hittawe, M.M.; Sun, Y. *Road Traffic Modeling and Management*; Elsevier: Amsterdam, The Netherlands, 2022. [CrossRef]
26. He, K.; Zhang, X.; Ren, S.; Sun, J. Deep Residual Learning for Image Recognition. In Proceedings of the IEEE Conference on Computer Vision and Pattern Recognition, Las Vegas, NV, USA, 27–30 June 2016; pp. 770–778. [CrossRef]

27. Hittawe, M.M.; Langodan, S.; Beya, O.; Hoteit, I.; Knio, O. Efficient SST Prediction in the Red Sea Using Hybrid Deep Learning-Based Approach. In Proceedings of the 2022 IEEE 20th International Conference on Industrial Informatics (INDIN), Perth, Australia, 25–28 July 2022; pp. 107–114. [CrossRef]
28. Hittawe, M.M.; Sidibé, D.; Beya, O.; Mériaudeau, F. Machine Vision for Timber Grading Singularities Detection and Applications. *J. Electron. Imaging* **2017**, *26*, 063015. [CrossRef]
29. Zhang, J.; Qian, S.; Tan, C. Automated Bridge Surface Crack Detection and Segmentation Using Computer Vision-Based Deep Learning Model. *Eng. Appl. Artif. Intell.* **2022**, *115*, 105225. [CrossRef]
30. Xu, Y.; Zhou, Y.; Sekula, P.; Ding, L. Machine Learning in Construction: From Shallow to Deep Learning. *Dev. Built Environ.* **2021**, *6*, 100045. [CrossRef]
31. Bochkovskiy, A.; Wang, C.-Y.; Liao, H.-Y.M. YOLOv4: Optimal Speed and Accuracy of Object Detection. *arXiv* **2020**, arXiv:2004.10934.
32. Li, C.; Li, L.; Jiang, H.; Weng, K.; Geng, Y.; Li, L.; Ke, Z.; Li, Q.; Cheng, M.; Nie, W.; et al. YOLOv6: A Single-Stage Object Detection Framework for Industrial Applications. *arXiv* **2022**, arXiv:2209.02976.
33. Li, C.; Li, L.; Geng, Y.; Jiang, H.; Cheng, M.; Zhang, B.; Ke, Z.; Xu, X.; Chu, X. YOLOv6 v3.0: A Full-Scale Reloading. *arXiv* **2023**, arXiv:2301.05586.
34. Wang, C.-Y.; Bochkovskiy, A.; Liao, H.-Y.M. YOLOv7: Trainable Bag-of-Freebies Sets New State-of-the-Art for Real-Time Object Detectors. In Proceedings of the IEEE/CVF Conference on Computer Vision and Pattern Recognition, New Orleans, LA, USA, 18–24 June 2022.
35. He, K.; Gkioxari, G.; Dollár, P.; Girshick, R. Mask R-CNN. In Proceedings of the IEEE International Conference on Computer Vision, Venice, Italy, 22–29 October 2017.
36. Ansari, S.; Rennie, C.D.; Clark, S.P.; Seidou, O. IceMaskNet: River Ice Detection and Characterization Using Deep Learning Algorithms Applied to Aerial Photography. *Cold Reg. Sci. Technol.* **2021**, *189*, 103324. [CrossRef]
37. Zhang, H.; Qian, Z.; Tan, Y.; Xie, Y.; Li, M. Investigation of Pavement Crack Detection Based on Deep Learning Method Using Weakly Supervised Instance Segmentation Framework. *Constr. Build. Mater.* **2022**, *358*, 129117. [CrossRef]
38. Liu, F.; Liu, J.; Wang, L.; Al-Qadi, I.L. Multiple-Type Distress Detection in Asphalt Concrete Pavement Using Infrared Thermography and Deep Learning. *Autom. Constr.* **2024**, *161*, 105355. [CrossRef]
39. Baduge, S.K.; Thilakarathna, S.; Perera, J.S.; Ruwanpathirana, G.P.; Doyle, L.; Duckett, M.; Lee, J.; Saenda, J.; Mendis, P. Assessment of Crack Severity of Asphalt Pavements Using Deep Learning Algorithms and Geospatial System. *Constr. Build. Mater.* **2023**, *401*, 132684. [CrossRef]
40. Xiong, X.; Meng, A.; Lu, J.; Tan, Y.; Chen, B.; Tang, J.; Zhang, C.; Xiao, S.; Hu, J. Automatic Detection and Location of Pavement Internal Distresses from Ground Penetrating Radar Images Based on Deep Learning. *Constr. Build. Mater.* **2024**, *411*, 134483. [CrossRef]
41. Al-Huda, Z.; Peng, B.; Algburi, R.N.A.; Al-antari, M.A.; AL-Jarazi, R.; Zhai, D. A Hybrid Deep Learning Pavement Crack Semantic Segmentation. *Eng. Appl. Artif. Intell.* **2023**, *122*, 106142. [CrossRef]
42. Song, Q.; Liu, L.; Lu, N.; Zhang, Y.; Muniyandi, R.C.; An, Y. A Three-Stage Pavement Image Crack Detection Framework with Positive Sample Augmentation. *Eng. Appl. Artif. Intell.* **2024**, *129*, 107624. [CrossRef]
43. Ounpraseuth, S.T. Gaussian Processes for Machine Learning. *J. Am. Stat. Assoc.* **2008**, *103*, 429. [CrossRef]
44. Shai, S.; Shai, B. *Understanding Machine Learning from Theory to Algorithm*; Cambridge University: Cambridge, UK, 2014.
45. Ali, R.; Chuah, J.H.; Talip, M.S.A.; Mokhtar, N.; Shoaib, M.A. Crack Segmentation Network Using Additive Attention Gate—CSN-II. *Eng. Appl. Artif. Intell.* **2022**, *114*, 105130. [CrossRef]
46. Vishwakarma, R.; Vennelakanti, R. CNN Model Tuning for Global Road Damage Detection. In Proceedings of the 2020 IEEE International Conference on Big Data, Atlanta, GA, USA, 10–13 December 2020; pp. 5609–5615. [CrossRef]
47. Pham, V.; Pham, C.; Dang, T. Road Damage Detection and Classification with Detectron2 and Faster R-CNN. In Proceedings of the 2020 IEEE International Conference on Big Data, Atlanta, GA, USA, 10–13 December 2020; pp. 5592–5601. [CrossRef]
48. Wu, Y.; Kirillov, A.; Massa, F.; Lo, W.; Girshick, R. Detectron2. Available online: https://github.com/facebookresearch/detectron2 (accessed on 15 May 2024).
49. Mokhtar, M.M.; Morsy, M.; Taha, N.A.; Ahmed, E.M. Investigating the Mechanical Performance of Nano Additives Reinforced High-Performance Concrete. *Constr. Build. Mater.* **2022**, *320*, 125537. [CrossRef]
50. Buslaev, A.; Iglovikov, V.I.; Khvedchenya, E.; Parinov, A.; Druzhinin, M.; Kalinin, A.A. Albumentations: Fast and Flexible Image Augmentations. *Information* **2020**, *11*, 125. [CrossRef]
51. Lee, S.Y.; Jeon, J.S.; Le, T.H.M. Feasibility of Automated Black Ice Segmentation in Various Climate Conditions Using Deep Learning. *Buildings* **2023**, *13*, 767. [CrossRef]
52. Singh, J.; Shekhar, S. Road Damage Detection and Classification in Smartphone Captured Images Using Mask R-CNN. *arXiv* **2018**, arXiv:1811.04535.
53. Ultralytics Ultralytics YOLOv8. Available online: https://docs.ultralytics.com/vi (accessed on 12 June 2024).
54. Zhang, Z.; Sabuncu, M.R. Generalized Cross Entropy Loss for Noisy Labels. Available online: https://neurips.cc/media/nips-2018/Slides/12761.pdf (accessed on 12 June 2024).

55. Nar, K.; Ocal, O.; Sastry, S.S.; Ramchandran, K. Cross-Entropy Loss and Low-Rank Features Have Responsibility for Adversarial Examples. *arXiv* **2019**, arXiv:1901.08360.
56. Figiel, Ł.; Kamiński, M. Numerical Probabilistic Approach to Sensitivity Analysis in a Fatigue Delamination Problem of a Two Layer Composite. *Appl. Math. Comput.* **2009**, *209*, 75–90. [CrossRef]

Disclaimer/Publisher's Note: The statements, opinions and data contained in all publications are solely those of the individual author(s) and contributor(s) and not of MDPI and/or the editor(s). MDPI and/or the editor(s) disclaim responsibility for any injury to people or property resulting from any ideas, methods, instructions or products referred to in the content.